Oniom (MP2:PM3) Study of C_{60}–Water Complex

LIOUDMILA FOMINA, ABRAHAM REYES, PATRICIA GUADARRAMA, SERGUEI FOMINE

Instituto de Investigaciones en Materiales, Universidad Nacional Autónoma de México, Apartado Postal 70-360, CU, Coyoacan, México DF 04510, México

Received 18 March 2003; accepted 3 June 2003

DOI 10.1002/qua.10761

ABSTRACT: The ONIOM (MP2:PM3) model in combination with local implementation of MP2 single-point energy evaluation was used to model the C_{60}–water complex. In agreement with experimental data, stabilization of the complex can be described in terms of interaction between the lone electron pair of water oxygen and π^*-orbitals of fullerene with electron correlation being the most important contribution to the complex stabilization. It was found that for qualitatively correct description of C_{60}–water complex geometry it is essential to have at least 12 carbon atoms of C_{60} molecule and water molecule in high MP2 ONIOM layer and use a basis set of at least 6-31+G(*d*,*p*) quality. © 2003 Wiley Periodicals, Inc. Int J Quantum Chem 97: 679–687, 2004

Key words: fullerene; local MP2 theory; van der Waals complexes; ONIOM

Introduction

Recently, many donor–acceptor complexes containing fullerenes have been prepared [1–12]. Electronic absorption spectra of some of these show charge transfer (CT) bands so that these compounds can be considered charge transfer complexes (CTCs) [2–9]. In most cases C_{60} CTC are neutral insulating compounds in which C_{60} cocrystallizes with donor molecules. Only strong electron donors like decamethylnickelocene, Fe(C_5H5)(C_6Me_6), cobaltocene, or tetrakis(dimethylamino)-ethylene produce ion-radical salts with C_{60} [13–15].

C_{60} also forms CTC with polymers bearing electron donor groups like polyvinylcarbazole, polythiophenes, and polyparaphenylenevinylenes [16, 17]. Similarly to many weak CT polymeric complexes they show high photoconductivity due to photoinduced electron transfer from a polymer to a C_{60} molecule forming metastable C_{60} anions and mobile holes in the polymer [16]. This property of polymeric CT fullerene complexes is currently of a great interest because these materials can be uti-

Correspondence to: S. Fomine; e-mail: fomine@servidor.unam.mx

lized in xerography, energy phototransducers, and molecular switches [18].

As recently shown C_{60} also forms complexes with water molecules [19, 20]. These complexes show biologic activity and appear promising in context of therapeutic applications. Thus, microdosis of hydrated fullerenes are effective in the treatment of oncological pathologies [21]. As follows from VIS absorbance spectra C_{60}–water complexes show two broad low-intensive bands at 450 and 600 nm [20]. The occurrence of such absorbance bands in the VIS region is known to be connected with formation of weak donor–acceptor complexes of C_{60} with molecules, which are able to be the donors of electrons, e.g., alcohols, aromatic rings, tertiary amines, and poly(vinylpyrrolidone) [22, 23]. According to this experimental data the geometry of C_{60}–water complexes must be different from that observed for water complexes with small aromatic molecules as benzene where π–H interaction exists [24].

Despite the great interest in fullerene CT complexes, few articles dealing with molecular modeling of these complexes have been published to date to the best of our knowledge. This is no surprise because the modeling of van der Waals interactions with reasonable accuracy requires at least the MP2 level of theory with a polarizable basis set, which is still out of reach for computational chemists in the case of such large molecules.

As confirmation of the fact that in CT complexes consisting of large molecules the closest atoms contribute most to the interaction energy, the ONIOM two-layer method has recently been successfully adopted by the present authors to study C_{60} complexes with simple donor molecules where donor molecules and 12 carbons of the naphthacene fragment of C_{60} were treated at the MP2/6-31G(*d*) level while for the rest of them the PM3 model was applied [25]. Local MP2 approximation was used to evaluate the binding energy of these CT complexes. Reduced step dependence of the computational cost on the size of molecule and reduced basis set superposition error (BSSE) are two important advantages of local MP2 method (LMP2) [26]. This approach was shown to be efficient for modeling of large C_{60} containing van der Waals complexes at reduced computational costs.

The goal of this article is to apply ONIOM (MP2: PM3) model in combination with LMP2 single-point energy evaluation to model the C_{60}–H_2O complex to get deeper insight into the nature of such an important system as well as test the applicability of the ONIOM model to study large van der Waals complexes.

Computational Details

All ONIOM optimizations were carried out using the Gaussian 98 suite of programs [27]. LMP2/3-21G optimization was carried out with Jaguar 4.2 package [28]. To obtain full picture of the applicability of the ONIOM (MP2:PM3) model to study the C_{60}–H_2O complex the following methodology has been adopted. Six different ONIOM C_{60}–H_2O systems were chosen, each having different numbers of atoms treated at the MP2 level.

The applicability of the MP2/3-21G model to geometry optimization was tested for the benzene–H_2O complex by comparison of optimized geometry with that obtained at the MP2/aug-cc-pVDZ level [29]. Geometries of the benzene–H_2O complex given by these two models were close (within 0.03 Å and 2° for distances and angles, respectively). One of the advantages of using the 3-21G basis set is the possibility of full optimization of the C_{60}–H_2O complex at the LMP2/3-21G level to obtain a reference point for discussion of ONIOM optimization results. Therefore, the MP2/3-21G level was adopted for high ONIOM layer as the lowest-level MP2 method. Three more basis sets [6-31G(*d*), 6-31+G(*d*,*p*), and 6-311+G(*d*,*p*)] were used for the MP2 layer to study the basis set quality effect on the molecular complex geometry and binding energies. They were used to model first four and three systems, respectively. Single-point energy calculation using local MP2 theory and the 6-311+G(*d*,*p*) basis set was used to calculate binding energy of the C_{60}–water complex using the Jaguar 4.2 package. LMP2 is already designed to avoid BSSE; therefore, only the Hartree–Fock (HF) counterpoise correction term has been computed according to Ref. [30].

To distinguish between different models for the C_{60}–H_2O complex, the following abbreviations have been adopted: **CN/basis set,** where N is the number of carbon atoms of C_{60} treated at the MP2 level and the 3-21G basis set is abbreviated as 321, 6-31G(*d*) as 631*d*, 6-31+G(*d*,*p*) as 631*dp*+, and 6-311+G(*d*,*p*) as 6311*dp*+. Note that the water molecule has always been treated at the MP2 level. The complex geometries are shown in Figures 1–4 where the water molecule interacts with the hexagon of the C_{60} molecule. Two types of initial geometries were tested. The first is similar to the C_{2v} benzene–H_2O complex with O—H bonds pointing

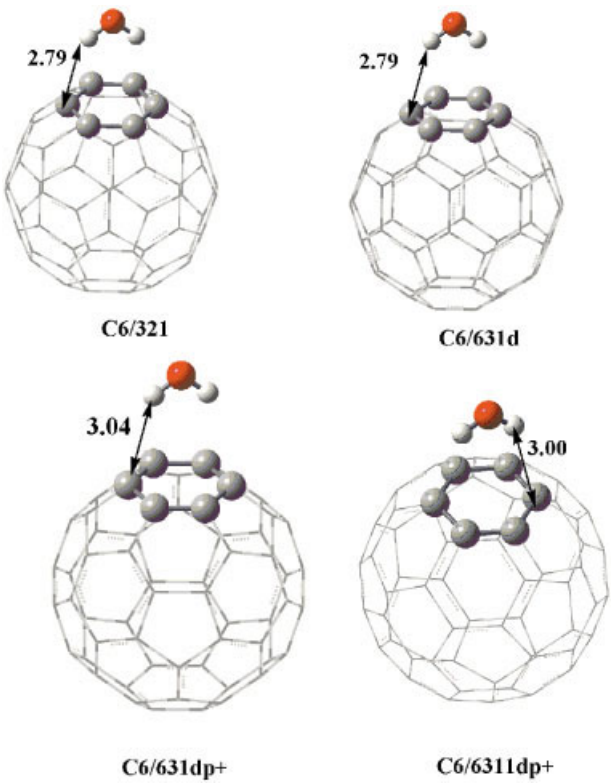

FIGURE 1. ONIOM optimized geometries of **C6** C_{60}–water complexes (ball-&-stick and wireframe rendering show MP2 and PM3 layers of ONIOM level, respectively). Selected distances are in Å. [Color figure can be viewed in the online issue, which is available at www.interscience.wiley.com.]

to hexagon. In the second type, the water molecule is rotated by 180° with the oxygen atom pointing toward the hexagon center.

Results and Discussion

It has recently been shown [25] that C_{60} complexes with simple donor molecules like dimethyl ether, dimethyl sulfide, and dimethylamine were stabilized mainly by electron correlation with slight charge transfer from the donor molecule to C_{60} through the interaction of donor highest occupied molecular orbital (HOMO) with the lowest unoccupied molecular orbital (LUMO) of C_{60}. The lone pair of a heteroatom is pointed to the center of a hexagon interacting with π^*-orbitals of fullerene. On the other hand, all available studies on the water–benzene complexes predict the existence of π–H interactions. In other words, benzene acts as a donor donating π-electrons to σ^*-orbitals of the HO bond of the water molecule [29]. The smallest basis set used for the MP2 ONIOM layer was 3-21G. Although double-split basis is too small for energy evaluations, it has been shown that a basis set of similar quality (6-31G) performs well in the case of naphthalene dimer optimizations [31].

ONIOM (MP2/3-21G:PM3) MODEL

Figures 1–4 show geometry of C_{60}–H_2O complexes optimized at different theoretical levels. Table I presents binding energies obtained using different theoretical models. Although we were able to extend the high MP2 layer of treatment to the entire complex for the 3-21 basis set, the most computationally demanding job—full MP2/3-21G optimization of the C_{60}–H_2O complex—had to be run at local MP2 approximation.

When examining Table I and Figures 1–4 one can observe a clear correlation between ONIOM binding energies, oxygen—C_{60} distance, and the number of atoms included in the high MP2 layer start-

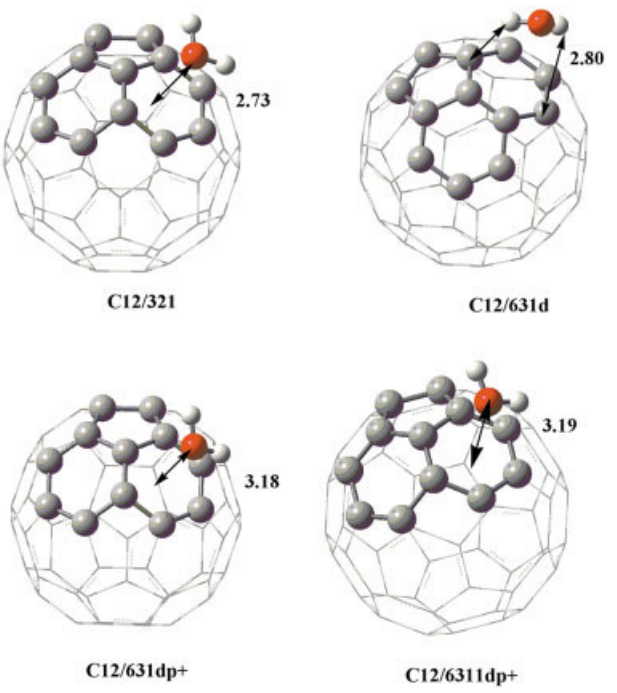

FIGURE 2. ONIOM optimized geometries of the **C12** C_{60}–water complex (ball-&-stick and wireframe rendering show MP2 and PM3 layers of ONIOM level, respectively). Selected distances are in Å. [Color figure can be viewed in the online issue, which is available at www.interscience.wiley.com.]

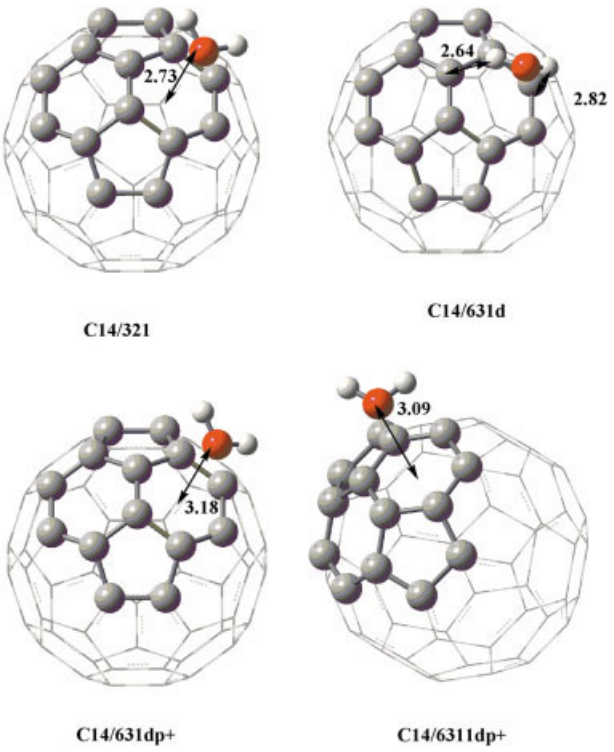

FIGURE 3. ONIOM optimized geometries of the **C14** C_{60}–water complex (ball-&-stick and wireframe rendering show MP2 and PM3 layers of ONIOM level, respectively). Selected distances are in Å [Color figure can be viewed in the online issue, which is available at www.interscience.wiley.com.]

ing from the **C12/321** model. The only exception is the **C_{60}/321** model due to local implementation of the MP2 theory for this case. There were observed qualitative changes in the geometry of complex when passing from **C6/321** to **C12/321.** As can be seen from Figure 1 model **C6/321** predicts π–H interaction similar to that found in benzene–water complexes where the C_{60} molecule acts as a donor. This is not the case for **C12/321** and all other **321** models where the oxygen atom, and not OH bonds, points to the C_{60} molecule, which can be described in terms of interaction of a water lone pair with π^*-orbitals of C_{60}. In the latter case C_{60} behaves as an acceptor. This explanation can be further confirmed inspecting Table II, where $LUMO_{H_2O}$-$HOMO_{C_{60}}$ and $LUMO_{C_{60}}$-$HOMO_{H_2O}$ energy gaps are listed. $HOMO_{C_{60}}$ and $LUMO_{C_{60}}$ are π- and π^*-orbitals, respectively, while $HOMO_{H_2O}$ and $LUMO_{H_2O}$ contribute p_x orbital of oxygen and σ^*-orbitals of the O—H bond. As seen from Table II the $LUMO_{C_{60}}$-$HOMO_{H_2O}$ energy difference for **C6/321** is larger compared to $LUMO_{H_2O}$-$HOMO_{C_{60}}$ while in all other **321** models the $LUMO_{H_2O}$-$HOMO_{C_{60}}$ energy difference is larger. This induces the reorientation of the water molecule in the C_{60}–H_2O complex for an MP2 layer larger than nine atoms at the MP2/3-21G level. An increase of ONIOM binding energies and shortening O-hexagon distance with expansion of MP2 layer are also in line with constant decrease in $LUMO_{C_{60}}$-$HOMO_{H_2O}$- energy gap in **C12/321–C48/321** models. This picture does not change qualitatively for the **C60/321** model, where complete LMP2/3-21G optimization is performed. The water molecule maintains its orientation and the overall complex geometry is simi-

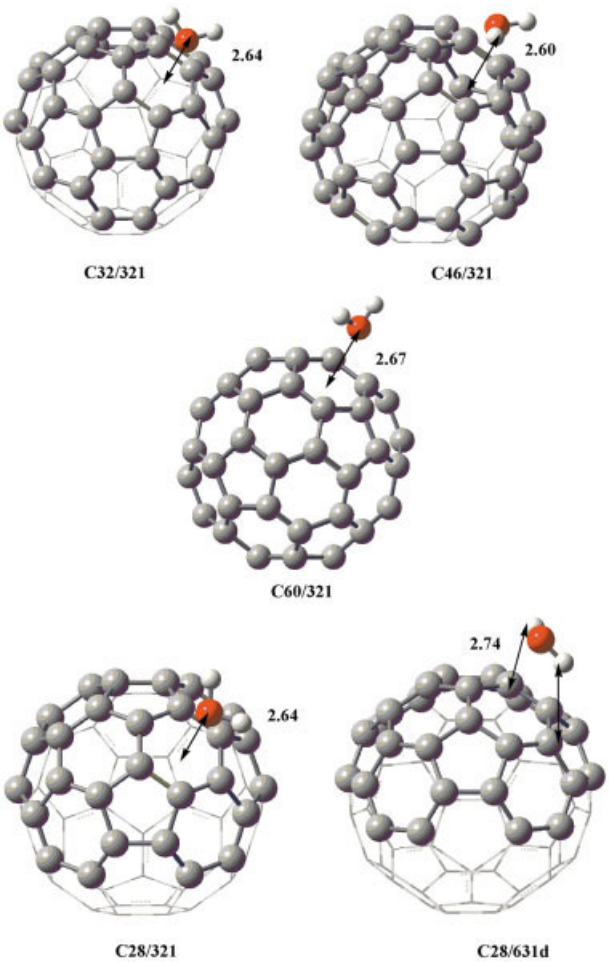

FIGURE 4. ONIOM optimized geometries of the highest **321** C_{60}–water complex (ball-&-stick and wireframe rendering show MP2 and PM3 layers of ONIOM level, respectively). Selected distances are in Å. [Color figure can be viewed in the online issue, which is available at www.interscience.wiley.com.]

TABLE I

Binding energies of C_{60}-water complexes at different levels of theory.

Model	SCF[a]	LMP2[b]	ONIOM[c]	$LMP2_{(corr)}$[d]	$SCF_{(corr)}$[e]	$\Delta E_{(corr)}$[f]
C6/321	1.06	−1.01	−2.77	−0.39	1.68	−2.07
C6/631*d*	1.14	−1.05	−2.77	−0.47	1.72	−2.19
C6/631*dp*+	0.00	−1.50	−2.10	−0.97	0.53	−1.50
C6/6311*dp*+	0.18	−1.48	−2.19	−0.98	0.68	−1.66
C12/321	3.64	0.95	−3.34	1.69	4.38	−2.69
C12/631*d*	1.75	−0.65	−3.16	−0.05	2.35	−2.40
C12/631*dp*+	0.47	−1.09	−3.60	−0.54	1.02	−1.56
C12/6311*dp*+	0.40	−1.12	−3.83	−0.52	1.00	−1.52
C14/321	3.70	0.93	−3.39	1.61	4.38	−2.77
C14/631*d*	1.53	−0.65	−3.23	0.11	2.29	−2.18
C14/631*dp*+	0.69	−0.93	−3.84	−0.64	0.98	−1.62
C14/6311*dp*+	0.92	−0.76	−3.34	−0.46	1.22	−1.68
C28/321	3.88	1.05	−4.32	2.08	4.91	−1.83
C28/631*d*	2.26	−0.10	3.49	0.6	2.96	−2.36
C32/321	3.86	1.05	−4.34	2.1	4.91	−2.81
C46/321	4.42	1.54	−5.01	2.25	5.13	−2.88
C60/321	3.83	−0.13	—	−0.35	3.61	−3.96

[a] Binding energy at the HF/6-311+G(*d*,*p*)//ONIOM level.
[b] Binding energy at the LMP2/6-311+G(*d*,*p*)//ONIOM level.
[c] ONIOM binding energy.
[d] BSSE-corrected binding energies at the LMP2/6-311+G(*d*,*p*)//ONIOM level.
[e] BSSE-corrected binding energies at the HF/6-311+G(*d*,*p*)//ONIOM level.
[f] Correlation stabilization of the C_{60}–water complex, defined as $[E_{AB}^{(LMP2)}-(E_{A}^{(LMP2)}-E_{B}^{(LMP2)})]-[E_{AB}^{(SCF)}-(E_{A}^{(SCF)}-E_{B}^{(SCF)})]$, where $E^{(SCF)}$ and $E^{(LMP2)}$ are SCF and LMP2 level energies of molecule A, B and molecular complex AB, respectively.

lar to those of **C12/321–C48/321** ones, in agreement with $LUMO_{H_2O}$-$HOMO_{C_{60}}$ and $LUMO_{C_{60}}$-$HOMO_{H_2O}$ energy differences. The hexagon—O distance decreases from 2.73 to 2.60 Å for **C12/321–C48/321** models, being 2.67 Å for **C60/321.**

Single-point stabilization energy calculation carried out at the LMP2/6-311+G(*d*,*p*) level of theory are listed in Table I. As can be seen BSSE is less than 1 kcal/mol due to the relatively large basis set used in calculations. Similar to the LMP2 study of naphthalene dimers [32] all **321** complexes are unstable at the HF level and the stabilizations are completely due to correlation energy. Unfortunately, we were not able to decompose HF contribution to stabilization energies using Kitaura–Morokuma decomposition schemes [33] due to difficulties to get the self-consistent field (SCF) converged for this analysis. However, some important conclusions can be made analyzing rough HF stabilization energies. As seen from Table I HF binding energy is less positive for the **C6/321** model, becoming significantly more positive for **C12/321,** and slightly increasing from **C12/321** to **C60/321.** This evolution of HF stabilization energies can be understood taking into account the results of HF binding energy partition performed for aromatic dimers [32]. Thus, the relatively small positive HF binding energy in the **C6/321** model is due to different from other **321** models water molecule orientation that contributes to additional stabilization at the HF level by H–π interactions (electrostatic term) and reduced exchange repulsion similar to that observed for *T*-shaped complexes of indole and naphthalene compared to parallel displaced ones [32]. Slight destabilization of **C12/321–C60/321** complexes at the HF level can be related to the increase in exchange repulsion with shortening of O–hexagon distance. There is no clear correlation in single-point energy between correlation contribution to the stabilization of **321** complexes and the number of atoms in the high MP2 ONIOM layer. The largest correlation stabilization was observed for the **C60/321** complex. Thus, only two of the **321** models predict negative stabilization energies at the LMP2/ONIOM level of theory: **C6/321** due to relatively small HF destabilization and **C60/321** due to large correlation stabilization.

TABLE II

Energy differences (Hartree) between LUMO of water and HOMO of C_{60} and LUMO of C_{60} and HOMO of water.

Model	$LUMO_{H_2O}$-$HOMO_{C_{60}}$	$LUMO_{C_{60}}$-$HOMO_{H_2O}$
C6		
321	0.58256	0.58535
631*d*	0.53074	0.60715
631*dp*+	0.47533	0.58553
6311*dp*+	0.47405	0.58575
C12		
321	0.53000	0.50451
631*d*	0.47849	0.53057
631*dp*+	0.42388	0.52277
6311*dp*+	0.42222	0.52227
C14		
321	0.50294	0.47267
631*d*	0.44976	0.50087
631*d*+	0.39580	0.49426
6311*dp*+	0.39462	0.49444
C28		
321	0.4679	0.42371
631*d*	0.41636	0.45793
C32		
321	0.46119	0.41326
631*d*		
C46		
321	0.48383	0.40076
C60		
321	0.56075	0.45114

SCF HOMO and LUMO energies of the MP2 layer of the C_{60} molecule optimized at the corresponding ONIOM level. SCF of HOMO and LUMO energies of the water molecule optimized at the MP2/3-21G, MP2/6-31G(*d*), MP2/6-31+G(*d*,*p*), and MP2/6-311+G(*d*,*p*) levels, respectively.

ONIOM [MP2/6-31G(*d*):PM3] MODEL

The use of the MP2/6-31G(*d*) model instead of MP2/3-21G for the high ONIOM layer significantly changed the complex geometry. Due to the larger size of jobs the maximum number of atoms included in the high ONIOM layer were 28 carbons of the C_{60} molecule and water [**C28/631*d***] model]. The molecular geometry of the C_{60}–water complex optimized making use of ONIOM [MP2/6-31G(*d*):PM3] model is shown in Figures 1–4. As can be seen from Figure 1 the basis set quality improvement does not affect the complex geometry for **C6** models. The geometries predicted by **C6/321** and **C6/631*d*** models are similar, with the OH bond pointing to the C_{60} hexagon with distances C—H of 2.79 Å. The situation changes for **C12/631*d*, C14/631*d*,** and **C28/631*d*** models. While all **321** models except **C6/321** predict that in the C_{60}–water complex the water oxygen points to fullerene hexagon, all **631*d*** models predict the complex geometry to be similar to **C6/321.**

As can be seen from Table II these differences in geometry owe to the differences in SCF MO energies. While in the ONIOM (MP2/3-21G:PM3) model the $LUMO_{C_{60}}$-$HOMO_{H_2O}$ energy gap is smaller compared to $LUMO_{H_2O}$-$HOMO_{C_{60}}$ for all complexes but **C6/321,** this is not the case for the ONIOM [MP2/6-31G(*d*):PM3] method, where for all models the $LUMO_{H_2O}$-$HOMO_{C_{60}}$ energy difference is less compared to $LUMO_{C_{60}}$-$HOMO_{H_2O}$. As a result all MP2/6-31G(*d*):PM3 models predict the C_{60}–water complex to be similar to **C6/321,** favoring $HOMO_{C_{60}}$-$LUMO_{H_2O}$ interactions.

The equilibrium geometry changes little with the number of atoms in the high MP2 layer for the ONIOM [MP2/6-31G(*d*):PM3] model, while ONIOM stabilization energies constantly increase, similar to ONIOM (MP2/3-21G:PM3), reaching −3.49 kcal/mol for **C28/631*d*.**

As can be seen from Table I the binding LMP2 energies calculated on ONIOM [MP2/6-31G(*d*):PM3] and ONIOM (MP2/3-21G:PM3) geometries are similar for **C6** models and different for the rest of them. Because ONIOM [MP2/6-31G(*d*):PM3] predicts the water molecule situated similar to that in the C_{2v} benzene–water complex, HF binding energies are less positive because of additional stabilization coming from π–H interactions and reduced exchange repulsion. On the other hand, the correlation stabilization is similar for two types of geometries, leading to better overall complex stabilization for ONIOM [MP2/6-31G(*d*):PM3] at the LMP2 level.

ONIOM [MP2/6-31+G(*d*,*p*):PM3] MODEL

Due to large job sizes, which implies the use of the ONIOM [MP2/6-31+G(*d*,*p*):PM3] model, the largest MP2 layer included only 14 C_{60} carbons and water molecule. Again, the geometry optimization results were different from these obtained for ONIOM [MP2/6-31G(*d*):PM3]. Thus, **C6/631*dp*+** predicts the complex to be qualitatively similar to **C6/631*d*** and **C6/321** ones with the OH bond pointing to the C_{60} hexagon (Fig. 1). The distances C—H in this case are longer (3.04 Å) compared to those obtained for **C6/631*d*** and **C6/321** models (2.79 Å). The ONIOM [MP2/6-31+G(*d*,*p*):PM3] model qual-

itatively reproduces the behavior of ONIOM (MP2/3-21G:PM3) with increased atom numbers in the high MP2 layer. Thus, as seen from Figures 2 and 3, **C12/631*dp*+** and **C14/631*dp*+** models are similar to **C12/3-21G** and **C14/3-21G** in terms of orientation of water molecules. These models predict for C_{60}–water complex the structure where the oxygen atom points to the center of the C_{60} hexagon. The difference is that **C12/631*dp*+** and **C14/631*dp*+** models predict the complex to be a bit looser compared to that predicted by **C12/3-21** and **C14/3-21.** Thus, the hexagon–O distance for **C12/631*dp*+** and **C14/631*dp*+** models (3.18 Å) is significantly larger compared to that (2.73–2.74 Å) for **C12/3-21G** and **C14/3-21G.** The reason for this change is not as obvious as in the case of ONIOM(MP2/3-21G:PM3). However, when carefully inspecting the evolution of $LUMO_{H_2O}$-$HOMO_{C_{60}}$ and $LUMO_{C_{60}}$-$HOMO_{H_2O}$ energy gaps with the number of atoms in the high MP2 layer one can observe that the $LUMO_{C_{60}}$-$HOMO_{H_2O}$ energy gap decrease faster compared to $LUMO_{H_2O}$-$HOMO_{C_{60}}$. This effect can revert at some point the relative stability of the first (**C6/631*dp*+**) and second (**C12/631*dp*+** and **C14/631*dp*+**) types of complexes at the MP2 level. Similar to all other models tested, the ONIOM stabilization energies become more negative with the number of atoms in MP2 atoms. As for LMP2 stabilization energies ONIOM [MP2/6-31+G(*d*,*p*):PM3] geometries produce the most stable C_{60}–water molecule at the LMP2 level. When inspecting Table I one can observe that SCF binding energies are always less positive compared to the two discussed models. This is definitely due to reduced exchange repulsion, which is a consequence of loose complex structure. On the other hand, this loose complex structure reduces correlation stabilization of **631*dp*+** complexes. However, the stability gain caused by reduction of exchange repulsion outweighs the destabilization caused by the drop in correlation stabilization, thus resulting in overall stabilization of the C_{60}–water complex.

ONIOM [MP2/6-311+G(*d*,*p*):PM3] MODEL

Similar to the ONIOM [MP2/6-31+G(*d*,*p*):PM3] model, ONIOM [MP2/6-311+G(*d*,*p*):PM3] was only practical for **C6, C12,** and **C14** systems due to the large basis set used in the high MP2 layer. In this case the overall geometry of the C_{60}–water complex follows the trend observed for **321** and **631*dp*+** models and differed from **631*d*.** Similar to these two methods, the **C6** model predicts existence of π–H interaction, while **C12** and **C14** models favor the complex where the lone pair of the oxygen atom interacts with π^*-orbitals of fullerene (Figs. 1, 2, and 3). As can be seen from these figures **631*dp*+** and **6311*dp*+** models predict geometries for the C_{60}–water complex similar to that of **6311*dp*+.** As follows from Table II the reasoning for the reorientation of the water molecule passing from **C6/6311*dp*+** to **C12/6311*dp*+** is similar to that given for **631*dp*+.**

ONIOM stabilization energies follow the same trend observed for all other models, predicting the complex to be more stable as the number of atoms in the high ONIOM level increases. LMP2 stabilization energies of the C_{60}–water complex predicted by ONIOM [MP2/6-311+G(*d*,*p*):PM3] are close to those calculated for ONIOM [MP2/6-311+G(*d*,*p*):PM3], one definitely showing basis set "saturation."

Comparison of Different Models

Because the only available experimental data that can be used for C_{60}–water complex geometry determination are those based on their electronic spectra [20]; no quantitative comparison with theoretical results can be made. However, qualitative comparison between modeling results and experimental observations is possible. As follows from VIS absorbance spectra, C_{60}–water complexes show two broad low-intensive bands at 450 and 600 nm [20]. The occurrence of such absorbance bands in the VIS region is known to be connected with the formation of weak donor–acceptor complexes of C_{60} with molecules, which are able to be the donors of electrons, e.g., alcohols, aromatic rings, tertiary amines, and poly(vinylpyrrolidone) [22, 23]. These data unambiguously favor a complex structure with the oxygen atom pointing to the fullerene molecule and can be understood taking into account the high electron affinity of the C_{60} molecule [34], unlike small aromatic molecules such as benzene acting as electron donor in complexes with water. Analyzing the four ONIOM models used in this study, one can see that the three using 3-21G, 6-31+G(*d*,*p*), and 6-311+G(*d*,*p*) are in qualitative agreement with experimental data starting from **C12** models. On the other hand, all **C6** ONIOM models and those using the 6-31G(*d*) basis set lead to qualitatively wrong conclusions about the complex geometry predicting water hydrogen pointing to the C_{60} molecule. The first case is easy to understand taking into account the fact that in all **C6**

models only six fullerene atoms are treated at the level proper for modeling of van der Waals interaction. On the other hand, it is clearly seen that relatively large basis sets with diffuse functions and at least 12 carbons in the high layer are needed to reproduce correctly the geometry of the C_{60}–water complex.

The ONIOM (MP2/3-21G:PM3) model describes the C_{60}–water complex surprisingly well, qualitatively reproducing trends of such high-level models as ONIOM [MP2/6-31+G(*d*,*p*):PM3] and ONIOM [MP2/6-311+G(*d*,*p*):PM3] while the better ONIOM [MP2/6-31G(*d*):PM3] completely fails to reproduce experimental geometry. The reason for such good performance of the 3-21G basis set is not obvious and probably related to the cancellation of errors leading to correct qualitative description of C_{60}–water complex geometry.

There are no experimental stabilization energies available for the C_{60}–water complex to compare them with calculated ones; therefore, comparison can only be made between different theoretical models. Because single-point energy evaluation of C_{60}–water complexes was carried out at reasonably high theoretical level, one can conclude that more negative stabilization energies correspond to more reasonably complex geometry. Thus, the ONIOM (MP2/3-21G:PM3) model, although succeeding to reproduce qualitatively the complex geometry, predicts the C_{60}–water complex to be unstable at the LMP2 level except for **C60/321,** where local implementation of MP2 theory is used for geometry optimization. This fact clearly shows that the 3-21G basis set is not adequate for quantitative discussion of C_{60}–water complex stability. The most negative stabilization energies at the LMP2 level, not counting **C6** models, were found for **C14/631*d*+** (−0.64 kcal/mol). Similar stabilization energies were found for **C14/6311*d*+**, ***C12/631d+***, and **C12/6311*d*+** (Table I). All these models predict similar geometry for the C_{60}–water complex with O—hexagon distance ranging from 3.19–3.09 Å.

Conclusions

It seems that the ONIOM (MP2:PM3) model in combination with LMP2 energy evaluation is a promising tool for modeling of large van der Waals complexes similar to the C_{60}–water one. To reproduce qualitatively correct C_{60}–water complex geometry at least 12 C_{60} carbons should be included in high MP2 level in combination with at least the 6-31+G(*d*,*p*) basis set. Calculations showed that the C_{60}–water complex is stabilized by the interaction of the lone pair of the water oxygen with π^*-orbitals of the C_{60} molecule, in agreement with experimental data [20].

Although ONIOM (MP2/3-21G:PM3) describes C_{60}–water complex geometry qualitatively correct, the reason for such good performance of the 3-21G basis set is not obvious. This could be related to the cancellation of errors leading to correct qualitative description of C_{60}–water complex geometry.

According to calculations, the most negative stabilization energy at the LMP2 level for models giving correct molecular geometry were found for the **C14/631*d*+** model (−0.64 kcal/mol). Similar stabilization energies were found for **C14/6311*d*+**, ***C12/631d+***, and **C12/6311*d*+** models (Table I). All these models predict similar geometry for the C_{60}–water complex with O—hexagon distance ranging from 3.19–3.09 Å and represent the most probable equilibrium structure for the C_{60}–water complex.

ACKNOWLEDGMENTS

This research was carried out with the support of Grants 33631-E and NC-204 from CONACyT.

References

1. Stephens, P. W.; Cox, D.; Lauher, J. W.; Mihaly, L.; Wiley, J. B.; Allemand, P.-M.; Hirsch, A.; Holczer, K.; Li, Q.; Thompson, J. D.; Wudl, F. Nature 1992, 355, 331.
2. Izuoka, A.; Tachikawa, T.; Sugawara, T.; Suzuki, Y.; Konno, M.; Saito, Y.; Shinohara, H. J Chem Soc Chem Commun 1992, 1472.
3. Saito, G.; Teramoto, T.; Otsuka, A.; Sugita, Y.; Ban, T.; Kusunoki, M.; Sakaguchi, K. I. Synth Met 1994, 64, 359.
4. Izuoka, A.; Tachikawa, T.; Sugawara, T.; Saito, Y.; Shinohara, H. Chem Lett 1992, 1049.
5. Llacay, J.; Tarres, J.; Veciana, J.; Rovira, C.; Veciana, J.; Mas, M.; Molins, E. J Phys Chem Solids 1997, 58, 1675.
6. Konarev, D. V.; Zubavichus, Y. V.; Slovokhotov, Y. L.; Shul'ga, Y. M.; Semkin, V. N.; Drichko, N. V.; Lyubovskaya, R. N.; Synth Met 1998, 92, 1.
7. Konarev, D. V.; Shul'ga, Y. M.; Roschupkina, O. S.; Lyubovskaya, R. N. J Phys Chem Solids 1997, 58, 1869.
8. Konarev, D. V.; Roschupkina, O. S.; Kaplunov, M. G.; Shul'ga, Y. M.; Yudanova, E. I.; Lyubovskaya, R. N. Mol Mater 1996, 8, 83.
9. Konarev, D. V.; Semkin, V. N.; Lyubovskaya, R. N.; Graja, A. Synth Met 1997, 88, 225.
10. Konarev, D. V.; Semkin, V. N.; Graja, A.; Lyubovskaya, R. N. J Mol Struct 1998, 450, 11.

11. Rao, C. N. R.; Govindaraj, A.; Sumathy, R.; Sood, A. K. Mol Phys 1996, 89, 267.
12. Nadtochenko, V. A.; Gritsenko, V. V.; D'yachenko, O. A.; Shilov, G. V.; Moravskii, A. P. Izv Akad Nauk Ser Khim 1996, 1285 (in Russian).
13. Bossard, C.; Rigaut, S.; Astruc, D.; Delville, M.; Felix, G.; Fevrier-Bouvier, A.; Amiell, J.; Flandrois, S.; Delhaes, P. J Chem Soc Chem Commun 1993, 333.
14. Stinchcombe, J.; Penicaud, A.; Bhyrappa, P.; Boyd, P. D. W.; Reed, C. A. J Am Chem Soc 1993, 115, 5212.
15. Allemand, P. M.; Khemani, K. C.; Koch, A.; Wudl, F.; Holczer, P. M.; Donovan, S.; Gruner, G.; Thompson, J. D. Science 1991, 253, 301.
16. Saricifti, N. S.; Smilowitz, L.; Heeger, A. J.; Wudl, F. Science 1992, 258, 1474.
17. Wang, Y. Nature, 1992, 356, 585.
18. Martyn, N.; Sanchez, L.; Illescas, B.; Perez, I. Chem Rev 1998, 98, 2527.
19. Deguchi, S.; Alargova, R. G.; Tsujii, K. Langmuir 2001, 17, 6013.
20. Andrievsky, G. V.; Klochkov, V. K.; Bordyuh, A. B.; Dovbeshko, G. I. Chem Phys Lett 2002, 364, 8.
21. Andrievsky, G. V.; Burenin, I. S.; Valueva, I. M.; Polyanskaya, N. I.; Borisova, L. M. In: Proceedings of the 5th Biennial International Workshop in Russia Fullerenes and Atomic Clusters; 2001; p. 345 (http://www.io.e.rssi.ru/IWFAC).
22. Hungerbühler, H.; Guldi, D. M.; Asmus, K.-D. J Am Chem Soc 1993, 115, 3386.
23. Ungurenasu, C.; Airinei, A. J Med Chem 2000, 43, 3186.
24. Suzuki, S.; Green, P. G.; Bumgarner, R. E.; Dasgurta, S.; Goddard, W. A. III; Blake, G. A. Science 1992, 257, 942.
25. Fomina, L.; Reyes, A.; Fomine, S. Int J Quantum Chem 2002, 89, 477.
26. Kim, K. S.; Tarakeshwar, P.; Lee, J. Y. Chem Rev 2000, 100, 4145.
27. Frisch, M. J.; Trucks, G. W.; Schlegel, H. B.; Scuseria, G. E.; Robb, M. A.; Cheeseman, J. R.; Zakrzewski, V. G.; Montgomery, J. A.; Stratmann, R. E. Jr.; Burant, J. C.; Dapprich, S.; Millam, J. M.; Daniels, A. D.; Kudin, K. N.; Strain, M. C.; Farkas, O.; Tomasi, J.; Barone, V.; Cossi, M.; Cammi, R.; Mennucci, B.; Pomelli, C.; Adamo, C.; Clifford, S.; Ochterski, J.; Petersson, G. A.; Ayala, P. Y.; Cui, Q.; Morokuma, K.; Malick, D. K.; Rabuck, A. D.; Raghavachari, K.; Foresman, J. B.; Cioslowski, J.; Ortiz, J. V.; Baboul, A. G.; Stefanov, B. B.; Liu, G.; Liashenko, A.; Piskorz, P.; Komaromi, I.; Gomperts, R.; Martin, R. L.; Fox, D. J.; Keith, T.; Al-Laham, M. A.; Peng, C. Y.; Nanayakkara, A.; Challacombe, M.; Gill, P. M. W.; Johnson, B.; Chen, W.; Wong, M. W.; Andres, J. L.; Gonzalez, C.; Head-Gordon, M.; Replogle, E. S.; Pople, J. A. Gaussian 98, revision A.9; Gaussian, Inc.: Pittsburgh, PA, 1998.
28. Jaguar 4.2; Schrodinger, Inc., Portland, OR, 2000.
29. Tarakeshwar, P.; Choi, H. S.; Lee, S. J.; Lee, J. Y.; Kim, K. S.; Ha, T. K.; Jang, J. H.; Lee, J. G.; Lee, H. J Phys Chem 1999, 111, 5838.
30. Boys, S. F.; Bernardi, F. Mol Phys 1970, 19, 553.
31. Gonzalez, C.; Lim, E. C. J Phys Chem A 1999, 103, 1437.
32. Fomine, S.; Tlenkopatchev, M.; Martinez, S.; Fomina, L. J Phys Chem 2002, 106, 3941.
33. Kitaura, K.; Morokuma, K. Int J Quantum Chem 1976, 10, 325.
34. Yang, S. H.; Pettiette, C. L.; Conceicao, J.; Cheshnovsky, O.; Smalley, R. E. Chem Phys Lett 1987, 139, 233.